2011 50th IEEE Conference on Decision and Control and
European Control Conference (CDC-ECC)
Orlando, FL, USA, December 12-15, 2011

Stabilizing and Robust FOPI Controller Synthesis for First Order Plus Time Delay Systems

Ying Luo[§], and YangQuan Chen[‡]

***Index Terms*— Fractional order proportional integral controller, integer order proportional integral derivative controller, first order plus time delay system, stability region, robustness, flat phase.**

***Abstract*— For all first order plus time delay (FOPTD) systems, a fractional order PI (FOPI) or a traditional integer order PID (IOPID) controller can be designed to fulfill three design specifications: gain crossover frequency, phase margin, and a flat phase constraint simultaneously. In this paper, a guideline for choosing feasible or achievable gain crossover frequency and phase margin specifications, and a new FOPI/IOPID controller synthesis are proposed for all FOPTD systems. Using this synthesis scheme, the complete feasible region of the gain crossover frequency and phase margin can be obtained and visualized in the plane. With this region as the prior knowledge, all combinations of the phase margin and gain crossover frequency can be verified before the controller design. Only if the combination is chosen from this achievable region, the existence of the stabilizing and desired FOPI/IOPID controller design can be guaranteed. Especially, it is interesting to compare the areas of these two feasible regions for the IOPID controller and the FOPI controller. This area comparison reveals, for the first time, the potential advantages of one controller over the other in terms of achievable performances. As a basic step, a scheme for finding the stabilizing region of the FOPI/IOPID controller is presented first, and then a new scheme for designing a stabilizing FOPI/IOPID controller satisfying the given gain crossover frequency, phase margin and flat phase constraint is proposed in details. Thereafter, the complete information about the feasible region of gain crossover frequency and phase margin is collected. This feasible region for the FOPI controller is compared with that for the traditional IOPID controller. This area comparison shows the advantage of the FOPI over the traditional IOPID clearly. Simulation illustration is presented to show the effectiveness and the performance of the designed FOPI controller comparing with the designed IOPID controller following the same synthesis in this paper.**

I. INTRODUCTION

Due to the relatively simple structure and remarkable effectiveness of implementation, the PID controllers are so far overwhelmingly applied in industrial applications [1]. It has been reported that, more than 95% of the control loops in process control industry are controlled by the PID controllers [2]. In the past decides, many techniques on design and tuning of the PID controllers are proposed. Some of the most popular methods are Ziegler-Nichols method [3], Cohen-Coon rule [4], modified Ziegler-Nichols scheme [3], integral performance criteria [5], Astrom-Hagglund method [1], and so on. Meanwhile, in order to improve the feedback control performance, variant PID controllers have been proposed, for typical examples, PID-dead time controller [6], IMC-PID controller [7], Smith predictor-PID controller [8], etc. In recent years, as the development of the fractional calculus theory [9] and the computer technology, the implementation of the fractional order controller has become feasible. The fractional order PID controllers have been proposed [10] and have received more and more attentions [11][12]. Some synthesis schemes for the fractional order PID controller in feedback control systems are presented in [11], these results showed the potential of the fractional order controllers to improve both the stability and robustness of the feedback control systems.

§ Department of Automation Science and Engineering, South China University of Technology, Guangzhou, P. R. China; Department of Electrical and Computer Engineering, Utah State University, Logan, UT, USA;
‡ Department of Electrical and Computer Engineering, Utah State University, Logan, UT 84322, USA.

The primary concern for the controller design and tuning is to maintain the stability of the control system. Stability is the minimal requirement for the controller design. Whereafter, some specific controller need to be determined to meet the desired robustness and performance criteria by searching over the stabilizing controller set. Recently, several schemes have been proposed to analyze the stability region for the traditional integer order PID controllers [13], and also for the fractional order PID controllers [14]. Within the complete stabilizing set, it is important to design the proper controllers to guarantee the robust requirement, and satisfy performance specifications, e.g., phase margin, gain margin, gain crossover frequency, etc. However, a proper controller may not be available or feasible for satisfying some performance requirements and robustness constraints, simultaneously.

For all first order plus time delay (FOPTD) systems, a controller can be designed to satisfy the given crossover frequency, phase margin and a flat phase constraint. This flat phase means that the system open loop phase is a constant around the given gain crossover frequency, which can show the iso-damping property for the system response. This scheme has been discussed in a previous work [11].

However, how do we know a selected combination of gain crossover frequency and phase margin is achievable for a proper controller while maintaining the flat phase feature? And is this designed controller stable? In this paper, in order to find a guideline for choosing the proper gain crossover frequency and phase margin to achieve a stabilizing and desired controllers, a new FOPI/IOPID controller design synthesis is proposed for all FOPTD systems.

Using this design scheme, a two dimension figure for the complete set of the feasible gain crossover frequency and phase margin can be drawn given any first order plus time delay system. With this complete set as the prior knowledge, all the combinations of phase margin and gain crossover frequency can be verified before the controller design. Only if the combination is chosen from this achievable region, the existence of the stabilizing and desired FOPI/IOPID can be guaranteed. Especially, it is interesting to compare the areas of these two feasible regions for the IOPID controller and the FOPI controller.

As a starting point, a scheme for finding the complete stabilizing region of the FOPI/IOPID controller for the given FOPTD system is presented, and then a new scheme for designing a stabilizing FOPI/IOPID controller satisfying the given gain crossover frequency, phase margin and flat phase constraint is proposed in details. After that, the complete feasible region of gain crossover frequency and phase margin is collected. This feasible region for the FOPI controller is compared with that for the traditional IOPID controller. This area comparison shows the advantage of the FOPI over the traditional IOPID clearly. Simulation illustration is presented to show the effectiveness and the performance of the designed FOPI controller comparing with the Ziegler-Nichols PID (ZNPID), and the designed IOPID controller following the same synthesis in this paper.

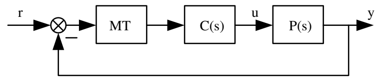

Fig. 1. Diagram of the feedback control system.

II. Stabilizing and Robust FOPI Controller Design for FOPTD Systems

A. The Plant and Controller Considered

Considering the feedback control system as shown in Fig. 1, $P(s)$ is the control plant, and $C(s)$ is the designed controller. The considered plant $P(s)$ in this paper is typically targeting the FOPTD systems, which are characterized by the following transfer function,

$$P(s) = \frac{K}{Ts+1}e^{-Ls}, \tag{1}$$

where, K represents the steady-state gain of the plant, T is the time constant, and L represents the time delay.

In this paper, in order to show the proposed controller synthesis clearly, we focus on the fractional order proportional integral (FOPI) controller $C(s)$ as follows,

$$C(s) = K_p + \frac{K_i}{s^r}, \tag{2}$$

where, K_p is the proportional gain, K_i is the integral gain, and the real number $r \in (0, 2)$ is the fractional order [9]. It is straightforward to extend this FOPI controller synthesis to the IOPID controller design case.

In Fig. 1, M_T is a Gain-Phase Margin Tester [15], which provides information for plotting the boundaries of constant gain margin and phase margin in the parameter plane [16]. The transfer function of M_T is given as,

$$M_T(A, \phi) = Ae^{-j\phi}. \tag{3}$$

Setting $\phi = 0$ in (3), the controller parameters boundary can be obtained satisfying a given gain margin A of the control system as shown in Fig. 1. Meanwhile, setting $A = 1$ in (3), one can get the controller parameters boundary for a given phase margin ϕ.

B. Stability Region Analysis of the FOPI Controller

The open-loop transfer function of the feedback control system in Fig. 1 can be derived from (1), (2), and (3),

$$G(s) = M_T(A, \phi)C(s)P(s). \tag{4}$$

The closed-loop transfer function can be expressed as,

$$T(s) = \frac{M_T(A, \phi)C(s)P(s)}{1 + M_T(A, \phi)C(s)P(s)}. \tag{5}$$

Substituting (1), (2), and (3) into (5), yields,

$$T(s) = \frac{Ae^{-j\phi}e^{-Ls}K(K_p s^r + K_i)}{s^r(Ts+1) + Ae^{-j\phi}e^{-Ls}K(K_p s^r + K_i)}. \tag{6}$$

Hence, the characteristic equation of the closed-loop system (5) is,

$$\begin{aligned} & D(K_p, K_i, r, A, \phi; s) \\ = \; & s^r(Ts+1) + Ae^{-j\phi}e^{-Ls}K(K_p s^r + K_i) = 0. \end{aligned} \tag{7}$$

The primary concern for the controller design is about the complete set of controllers which can stabilize the system. On the FOPI controller design for the FOPTD plants, the system stability is depending on the locations of the roots of the characteristic equation (7) with $A = 1$ and $\phi = 0°$. If all roots of the polynomial (7) are located in the left-half of the s-plane, the closed-loop system (5) is bounded-input bounded-output stable. There are three parameters K_p, K_i and r for the FOPI controller. The stability region Q of these three controller parameters is defined as that, if $(K_p, K_i, r) \in Q$, all the roots of $D(K_p, K_i, r, A, \phi; s)$ line in the left-half of the s-plane. The boundaries of the controller parameters stability region Q can be determined by the real root boundary (RRB) and complex root boundary (CRB) [17][18][13][16].

- Region of r: For the fractional order r in the FOPI controller, the chosen range is defined as $r \in (0, 2)$.
- RRB: The real root boundary is defined by the equation $D(K_p, K_i, r, A, \phi; s = 0) = 0$, so, one can get the boundary as, $K_i = 0$.
- CRB: Substituting $j\omega$ for s in (7), the complex root boundary can be defined from $D(K_p, K_i, r, A, \phi; s = j\omega) = 0$ as follows,

$$\begin{aligned} & D(K_p, K_i, r, A, \phi; j\omega) = (j\omega)^r(jT\omega + 1) \\ & + Ae^{-j\phi}e^{-j\omega L}K(K_p(j\omega)^r + K_i) \\ & = 0. \end{aligned} \tag{8}$$

Considering the real part and the imaginary part of (8) respectively, one can obtain,

$$\begin{aligned} & \omega^r \cos\frac{r\pi}{2} - T\omega^{1+r}\sin r\pi 2 \\ & + AK\cos(\phi + \omega L)(K_i + K_p\omega^r \cos r\pi 2) \\ & + AK\sin(\phi + \omega L)K_p\omega^r \sin r\pi 2 \\ & = 0; \end{aligned} \tag{9}$$

$$\begin{aligned} & T\omega^{1+r}\cos\frac{r\pi}{2} + \omega^r \sin r\pi 2 \\ & + AK\cos(\phi + \omega L)K_p\omega^r \sin r\pi 2 \\ & - AK\sin(\phi + \omega L)(K_i + K_p\omega^r \cos r\pi 2) \\ & = 0. \end{aligned} \tag{10}$$

From (9) and (10), it yields,

$$B_1 + AKC_1E + AKS_1F = 0, \tag{11}$$

$$B_2 + AKC_1F - AKS_1E = 0, \tag{12}$$

where,

$$\begin{aligned} B_1 &= \omega^r C_2 - T\omega^{1+r}S_2, \\ B_2 &= T\omega^{1+r}C_2 + \omega^r S_2, \\ C_1 &= \cos(\phi + \omega L), \quad S_1 = \sin(\phi + \omega L), \\ C_2 &= \cos\frac{r\pi}{2}, \quad S_2 = \sin\frac{r\pi}{2}, \\ E &= K_i + K_p\omega^r C_2, \quad F = K_p\omega^r S_2. \end{aligned}$$

From (11) and (12),

$$K_p = \frac{-(B_1S_1 + B_2C_1)}{AKS_2\omega^r}, \tag{13}$$

$$K_i = \frac{B - B_1S_1C_1 - B_2C_1^2}{AKS_1} + \frac{B_1S_1C_2 + B_2C_1C_2}{AKS_2}. \tag{14}$$

Hence, given r, the curve of K_i w. r. t. K_p can be plotted with $\omega \to +\infty$ from zero.

So, with $A = 1$, $\phi = 0°$ and a fixed fractional order r, the parameter-plane (K_p, K_i) is divided into stable and unstable regions by the RRB and CRB presented above. The stable region can be detected by testing one random point in every region [19]. Thus, the stability region of the parameters K_i and K_p can be fixed by the RRB and CRB conditions with a fixed r in the interval (0, 2). By sweeping over all the $r \in (0, 2)$, the three-dimension stability region in the parameter-space for the three parameters of FOPI can be determined, which is named as the *complete stability region*.

C. FOPI Parameters Design with Two Specifications

Since the *complete stability region* is determined, the special surface in the *complete stability region* can be drawn to satisfy the specified phase margin ϕ_m when we set $A = 1$ and $\phi = \phi_m$ in (8), or satisfy the specified gain margin A_m with the set of $\phi = 0°$ and $A = A_m$ in (8).

Given one specification $--$ phase margin ϕ_m, a *relative stability line* can be drawn in the (K_p, K_i)-plane as $\omega \to \omega_0$ from zero with a certain fixed $r_1 \in (0, 2)$, by setting $A = 1$ and $\phi = \phi_m$ in (8). ω_0 is the maximum frequency on the *relative stability line* and in the *complete stability region*. Sweeping all the r in $(0, 2)$, a surface in the three-dimension parameter-space can be generated satisfying the pre-specified ϕ_m. This surface is named as the *relative stability surface*. The maximum frequency ω_{0max} in all ω_0 on all *relative stability lines* with $r_1 \in (0, 2)$ is the frequency upper boundary of the *relative stability surface*.

Given another specification $--$ gain crossover frequency ω_c, a point corresponding to the parameters K_p and K_i on the *relative stability line* can be determined with a fixed r_1.

Actually, from (5) and (7), one can get characteristic equation of the closed-loop system (5),

$$1 + M_T(A, \phi)C(s)P(s)|_{s=j\omega} = 0,$$

which means the open-loop transfer function $G(s)$ is equal to -1 with $s = j\omega$,

$$G(s)_{s=j\omega} = M_T(A, \phi)C(s)P(s)|_{s=j\omega} = -1, \qquad (15)$$

so, one can get the magnitude equation,

$$|M_T(A, \phi)C(s)P(s)|_{s=j\omega}| = 1,$$

and the phase equation,

$$\angle(M_T(A, \phi)C(s)P(s)|_{s=j\omega}) = -\pi.$$

If setting $A = 1$ and $\phi = \phi_m$, all the $\omega \in (0, \omega_0]$ satisfying equation (15) can be treated as the gain crossover frequencies for the control system (5) in Fig. 1. Since the *relative stability lines* are generated from equation (7) which is equal to equation (15), all the frequency ω corresponding to the points on the *relative stability lines* can be treated as the gain crossover frequency.

So, with the pre-specified ω_c, ϕ_m and a fixed r_1, the other two FOPI parameters K_p and K_i can be determined on a point of the *relative stability lines*. In the same way, sweeping all the r in $(0, 2)$, a curve in the three-dimension parameter-space can be determined, which is the *relative stability curve*. All the points on this curve can guarantee the two pre-specifications ω_c and ϕ_m.

To make the FOPI controller parameter setting unique, we need one more specification.

D. FOPI Parameters Design with An Additional Flat Phase Constraint

In this section, an additional flat phase tuning constraint is presented to make the parameters of the FOPI controller unique.

From (11) and (12),

$$S_1 = \frac{B_2E - B_1F}{AK(E^2 + F^2)}, \quad C_1 = \frac{-B_1E - B_2F}{AK(E^2 + F^2)}, \qquad (16)$$

so, one can get,

$$\phi = \arctan\frac{B_1F - B_2E}{B_1E + B_2F} - \omega L + n\pi, \qquad (17)$$

where, n is an integer which guarantees,

$$\phi + \omega L - n\pi = \arctan\frac{B_1F - B_2E}{B_1E + B_2F} \in (-\pi/2, \pi/2).$$

In order to make the system robustness to the loop gain variations, the flat phase constraint as an additional specification is presented to design the FOPI controllers. The flat phase means the phase of the open-loop system is flat around the gain crossover frequency point in the Bode plot. With this constraint, the system phase can maintain almost the same value when the loop gain changes in a certain interval, namely, the system with this designed FOPI is robust to the loop gain variations, and the overshoots of the step responses are almost the same with the loop gain variations in certain range, which is called "iso-damping" property.

In order to satisfy the flat phase tuning constraint, the derivative of the open-loop phase θ w. r. t. the frequency ω is forced to be zero at the gain crossover frequency point, e.g., $\frac{\mathrm{d}\theta}{\mathrm{d}\omega} = 0$.

As mentioned in Sec. II-C, ϕ can be treated as the phase margin by setting $A = 1$ in (8). Thus, $\theta = \phi - \pi$, and, $\frac{\mathrm{d}\theta}{\mathrm{d}\omega} = \frac{\mathrm{d}\phi}{\mathrm{d}\omega} = 0$. From (17), one can get,

$$\frac{\mathrm{d}\phi}{\mathrm{d}\omega} = \frac{M}{(B_1E + B_2F)^2 + (B_1F - B_2E)^2} - L = 0,$$

$$M = (B_1^2 + B_2^2)(EF' - E'F) + (B_1'B_2 - B_1B_2')(E^2 + F^2),$$

where,

$$\begin{aligned} E' &= C_2K_pr\omega^{r-1}, \quad F' = S_2K_pr\omega^{r-1}, \\ B_1' &= C_2r\omega^{r-1} - S_2T(1 + r)\omega^r, \\ B_2' &= S_2r\omega^{r-1} + C_2T(1 + r)\omega^r. \end{aligned} \qquad (18)$$

From Sec. II-C, all FOPI parameter points on the *relative stability curve* in the three-dimension parameter-space satisfying both the pre-specified ϕ_m and ω_c, can be tested by the equation (18). If certain point with the FOPI parameters (K_p, K_i, r) on the r*elative stability curve* can be found to satisfy the relationship (18), this point is the *flat phase stable point*, which is the goal of this FOPI controller design for the given FOPTD system.

Thus, the FOPI controller from this *flat phase stable point* can achieve the desired control performance introduced by the two specifications ϕ_m and ω_c, and the robustness to the loop gain changes induced by the flat phase tuning constraint.

E. Achievable Region Collection of Two Specifications for FOPI Controller Design

From Sec. II-C, the upper boundary ω_{0max} of the gain crossover frequency specification can be found satisfying the given phase margin ϕ_m with a fixed r_1 in $(0, 2)$. Pre-specifying a phase margin ϕ_m, one *relative stability curve* in the three-dimension parameter-space can be detected for one $\omega_c \in (0, \omega_{0max}]$. The existence of the *flat phase stable point* can be detected on each *relative stability curve* with each ω_c.

So, with a fixed phase margin, the region for choosing the gain crossover frequency to get the desired FOPI controller can be decided by searching the frequency in between $(0, \omega_{0max}]$. Whereafter, sweeping the phase margin specification from 0 to 2π, the complete achievable region for the phase margin and gain crossover frequency, guaranteeing a FOPI controller satisfying the flat phase tuning constraint, can be collected.

According to this instructional information of the achievable region, a feasible combination of phase margin ϕ_m and gain crossover frequency ω_c can be checked in advance before controller design, and the desired stabilizing and robust FOPI controller can be designed following the proposed synthesis in this paper.

III. Design Procedures Summary with the Illustration of An Example

In this section, the procedures are summarized with the illustration of an examples for the proposed FOPI controller design.

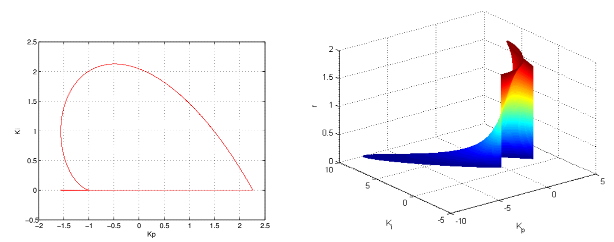

(a) Stability boundary of K_i w. r. t. K_p with r=0.5 (b) *Complete stability region* of K_i, K_p and r

Fig. 2. Stability boundary of K_i w. r. t. K_p with r=0.5 and *complete stability region*.

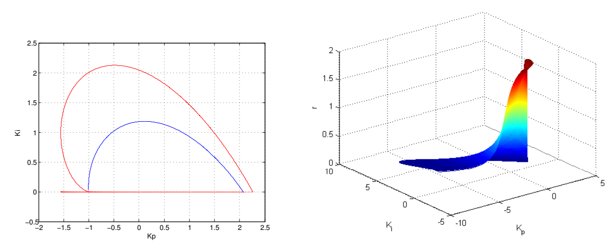

(a) Stability region comparison of K_i and K_p with $\phi_m = 0°$ in red line and $\phi_m = 50°$ in blue line ($r = 0.5$) (b) Three-dimension *relative stability surface* of K_i, K_p and r with $\phi_m = 50°$

Fig. 3. Stability boundary comparison of K_i and K_p and three-dimension *relative stability surface* with $\phi_m = 50°$.

Step 1: Given the first order plus time delay plant with $K = 1$, $T = 1s$ and $L = 1s$, and two specifications on the phase margin $\phi_m = 50°$ and gain crossover frequency $\omega_c = 0.5\ rad/s$.

Step 2: With the range of fractional order $r \in (0, 2)$, choose $r = 0.5$ and draw the line of K_p w. r. t. K_i in the (K_p, K_i)-plane according to the equations (13) and (14) of CRB in Sec. II-B. Draw the line $K_i = 0$ according to RRB in Sec. II-B. Detect the stabilizing region with random point test [19] as shown the red line boundary surrounded section in Fig. 2(a). Obtain the *complete stability region* as shown in Fig. 2(b) by sweeping all the r in $(0, 2)$, following the scheme introduced in Sec. II-B.

Step 3: With the pre-specified $\phi_m = 50°$ and fixed $r = 0.5$, the *relative stability line* in the (K_p, K_i)-plane can be drawn as the blue line in Fig. 3(a), which can be compared with the complete stability boundary as shown the red line. Get the *relative stability surface* by sweeping all r in $(0, 2)$ in Fig. 3(b) in the three-dimension parameter-space, satisfying the pre-specified phase margin $\phi_m = 50°$.

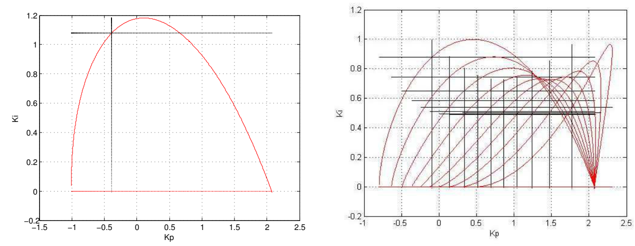

(a) With $r = 0.5$ (b) With sweeping all the optional $r \in (0, 2)$

Fig. 4. The designed K_i and K_p satisfying $\omega_c = 0.5\ rad/s$, $\phi_m = 50°$ with $r = 0.5$ and with sweeping all the optional $r \in (0, 2)$.

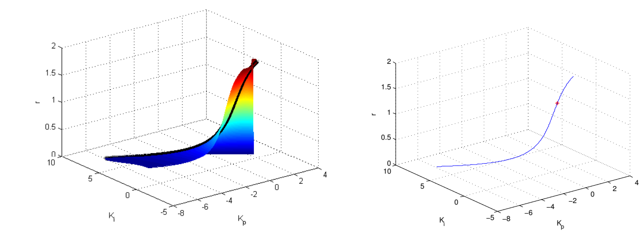

(a) The *relative stability curve* on the *relative stability surface* (b) The *flat phase stable point* on the *relative stability curve*

Fig. 5. The *relative stability curve* and the *flat phase stable point* in the three-dimension parameter-space.

According to the *relative stability surface* in Fig. 3(b), the maximum value ω_{0max} of ω_0 which is corresponding to the biggest frequency point on each *relative stability line* for different r, is $\omega_{0max} = 1.38\ rad/s$.

Step 4: Given gain crossover frequency $\omega_c = 0.5\ rad/s$, phase margin $\phi_m = 50°$ and $r = 0.5$, the other two parameters K_p and K_i can be determined from the intersection point in Fig. 4(a) with $\omega = \omega_c = 0.5\ rad/s$. Sweeping all the $r \in (0, 2)$ as shown in Fig. 4(b), one can get the *relative stability curve* presented as the black curve in Fig. 5(a) on the *relative stability surface* with $\phi_m = 50°$. All points on this *relative stability curve* can satisfy the two specifications $\phi_m = 50°$ and $\omega_c = 0.5\ rad/s$ simultaneously.

Step 5: Test all points on the *relative stability curve* to find a solution of equation (18), this point is illustrated as a red star on the *relative stability curve* in the three-dimension parameter-space of Fig. 5(b). This point is the *flat phase stable point*. Get the corresponding parameters (K_p, K_i, r) on this *flat phase stable point* to fix the FOPI controller satisfying the pre-specified phase margin, gain crossover frequency and the flat phase constraint.

IV. Complete Information Collection for Achievable Region of ω_c and ϕ_m

In order to high light the scheme of complete achievable region collection for the ω_c and ϕ_m, this procedure is separated from the procedures summary in Section III.

Step 6: With the frequency boundary ω_{0max} from *Step 3*, obtain the optional range of the gain crossover frequency $\omega_c \in (0, \omega_{0max}]$ under the pre-specified phase margin $\phi_m = 50°$. One *relative stability curve* can be drawn with one $\omega_c \in (0, \omega_{0max}]$ under $\phi_m = 50°$, and the existence of the *flat phase stabile point* can be test on each *relative stability curve*. So, the achievable gain crossover frequency ω_c for guaranteeing the existence of the *flat phase stable point* with $\phi_m = 50°$, can be collected. The achievable ω_c interval is corresponding to the nonzero solution of the *flat phase stable point* $(K_{pfp}, K_{ifp}, r_{fp})$. Testing different phase margin $\phi_m \in (0, 2\pi)$, the complete information for the achievable region of the specifications phase margin and gain crossover frequency, can be generated as shown the red region in Fig. 6(a).

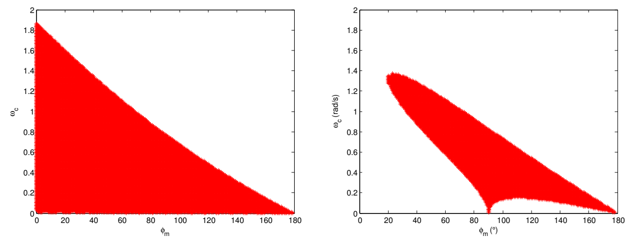

(a) FOPI with $T = 1s$ and $L = 1s$ (b) IOPID with $T = 1s$ and $L = 1s$

Fig. 6. The achievable region of ω_c and ϕ_m for FOPI and IOPID design with $T = 1s$ and $L = 1s$.

In order to show the advantages of the fractional order PI controller, the integer order PID (IOPID) controller is also designed with specifications on the phase margin, gain crossover frequency and flat phase requirement following the same synthesis in this paper.

Therefore, the complete achievable regions of the ϕ_m and ω_c are collected for IOPID with the given FOPTD setting $T = 1$ and $L = 1s$, as shown in Fig. 6(b).

From the comparisons of Fig. 6, it can be seen clearly that, the feasible region of ϕ_m and ω_c for FOPI is significantly bigger than that for IOPID. This bigger achievable region for FOPI over IOPID gives the users more capability and flexibility to design the proper controller and get the desired control performance. The advantage of the proposed FOPI controller over the traditional IOPID controller is illustrated clearly through these comparisons on the achievable regions of the two specifications.

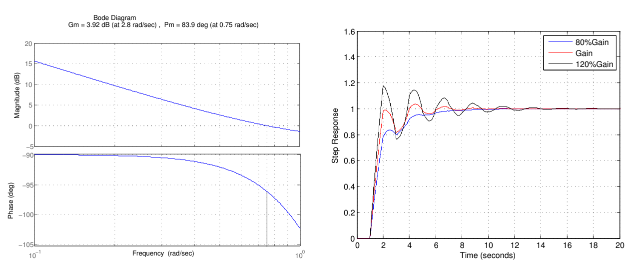

(a) Open-loop Bode plot (b) Step responses

Fig. 7. Open-loop Bode plot and step responses in continuous time domain with loop gain variations using the ZNPID controller.

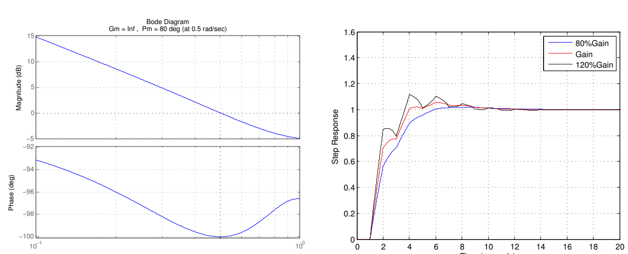

(a) Open-loop Bode plot (b) Step responses

Fig. 8. Open-loop Bode plot and step responses in continuous time domain with loop gain variations using the flat phase designed IOPID controller.

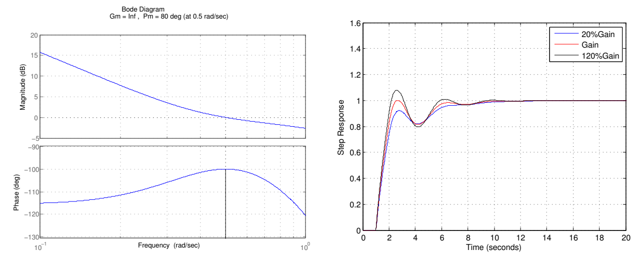

(a) Open-loop Bode plot (b) Step responses

Fig. 9. Open-loop Bode plot and discretized step responses with loop gain variations using the designed FOPI controller #1 C_{fopi21}.

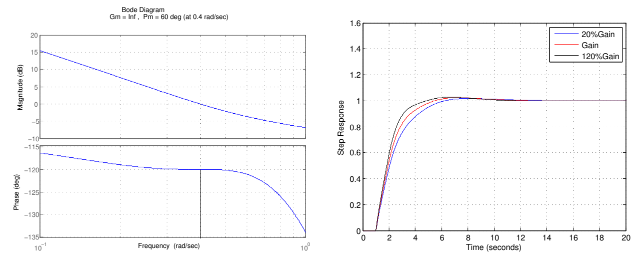

(a) Open-loop Bode plot (b) Step responses

Fig. 10. Open-loop Bode plot and discretized step responses with loop gain variations using the designed FOPI controller #2 C_{fopi22}.

V. SIMULATION ILLUSTRATION

In this section, the designed FOPI controller is validated by the numerical simulation illustration. In order to verify the effectiveness of this proposed controller design synthesis and show the advantages of the designed FOPI controller, the traditional Ziegler-Nichols PID (ZNPID) controller is designed, and the integer order PID (IOPID) controller is also designed following the same scheme in this paper. These designed two integer order controllers (ZNPID and IOPID) are compared with the designed FOPI controller for the given FOPTD model in the simulation.

The FOPTD simulation model (1) is chosen with $K = 1$, $T = 1s$ and $L = 1s$. According to the Ziegler-Nichols tuning rule [3] for the FOPTD systems, the ZNPID controller can be designed as,

$$C_{znpid2}(s) = K_{pzn2} + K_{izn2}\frac{1}{s} + K_{dzn2}s = 1.2 + 0.6\frac{1}{s} + 0.6s.$$

From the complete achievable region of the specifications in Fig. 6, the combination of $\omega_c = 0.5rad/s$ and $\phi_m = 80°$ are achievable for both IOPID and FOPI controllers. So, these two controllers can be designed as follows,

$$C_{iopid2}(s) = 0.7935 + \frac{0.5513}{s} + 0.6301s,$$

$$C_{fopi21}(s) = 1.1339 + \frac{0.3582}{s^{1.2597}}.$$

From Fig. 6, the combination of $\omega_c = 0.4rad/s$ and $\phi_m = 60°$ is achievable for the FOPI controller design, but not for the IOPID controller design. This shows the advantage of the FOPI controller over the traditional integer order PID controller. The stabilizing FOPI controller can be designed with the set of $\omega_c = 0.4rad/s$ and $\phi_m = 60°$, following the scheme in this paper,

$$C_{fopi22}(s) = 0.6727 + \frac{0.3597}{s^{1.2329}}.$$

With the given FOPTD model and the above four designed controllers, the Bode plots of the open-loop transfer functions can be drawn in Fig. 7(a), Fig. 8(a), Fig. 9(a), and Fig. 10(a), for the designed C_{znpid2}, C_{iopid2}, C_{fopi21} and C_{fopi22}, respectively. It can be seen that, all the Bode plots with the designed C_{iopid2}, C_{fopi21}, and C_{fopi22} satisfy the flat phase requirement and two corresponding specifications ω_c and ϕ_m.

In order to show the performance of the designed controllers, step responses are tested with loop gain variations. The Fig. 7(b) and Fig. 8(b) show the step responses using the designed C_{znpid2} and C_{iopid2} controllers, respectively, with the loop gain variations $\pm 20\%$.

The Fig. 9(b) and Fig. 10(b) show the step responses using the designed C_{fopi21} and C_{fopi22} controllers, respectively, with the loop gain variations $\pm 20\%$. The fractional order operators s^r is also implemented by the impulse response invariant discretization methods in time domain [20].

One can see that, the designed C_{iopid2}, C_{fopi21} and C_{fopi22} controller outperform the ZNPID controller C_{znpid2}, and the designed two FOPI controllers can get better performance than the designed traditional IOPID controller C_{iopid2}. C_{iopid2} and C_{fopi21} are both designed following the same specifications $\omega_c = 0.5\ rad/s$ and $\phi_m = 80°$. C_{iopid2} is designed with different specifications combination of $\omega_c = 0.45\ rad/s$ and $\phi_m = 60°$, which is beyond of the achievable region in Fig. 6(b) for IOPID controller design. It is obviously that, the performance using C_{iopid2} is the best over the other three designed controllers. More flexibility and capability for the FOPI controller design is illustrated by this simulation case.

VI. Conclusion

This paper provides a synthesis for the fractional order PI controllers to achieve two pre-specifications, e.g., phase margin and gain crossover frequency, and flat phase tuning constraint for the first order plus time systems. This designed FOPI controller can be stable for sure as its parameters are located in the *complete stability region*. This controller can get the desired control performance as satisfying two specifications. It can also be robust to the loop gain variations as following the flat phase constraint. Furthermore, the complete achievable region of the two specifications (phase margin and gain crossover frequency) can be collected for the FOPI controller design. This is an important benefit of this proposed design synthesis. The advantage of the FOPI controller is presented from the comparison of the achievable region of the two specifications over the IOPID controller. Simulation illustration is presented to show the performance and benefit of the designed FOPI controller comparing with traditional Ziegler-Nichols PID controller and the designed integer order PID controller following the same design scheme for the FOPI, based on the first order plus time delay plants.

VII. References

[1] K. Astrom and T. Hagglund, "Advanced PID Control," *Research Triangle Park, NC: ISA*, 2005.

[2] K. Astrom and T. Hagglund, "PID Controllers: Theory, Design and Tuning," *Instrument Society of America, Research Triangle Park*, 1995.

[3] J. G. Ziegler and N. B. Nichols, "Optimum setting for automatic controller," *Trans. ASME*, vol. 64, pp. 759–768, 1942.

[4] G. H. Cohen and G. A. Coon, "Theoretical consideration of retarded control," *Trans. Amer. Soc. Mech. Eng.*, vol. 75, pp. 827–834, 1953.

[5] C. A. Smith and A. B. Corripio, "Principles and practice of automatic process control," *New York: Wiley*, 1985.

[6] C. Hwang, J. H. Hwang, and L. F. Hwang, "Design of a PID-deadtime control for time-delay systems using the coefficient diagram method," *Journal of the Chinese Institute of Chemical Engineers*, vol. 33, no. 6, pp. 565–571, 2002.

[7] A. Leva and A. M. Colombo, "On the IMC base synthesis of the feedback block of ISA PID regulators," *Transactions of the Institute of Measurement and Control*, vol. 26, no. 5, pp. 417–440, 2004.

[8] O. J. M. Smith, "A controller to overcome dead time," *ISA Journal*, vol. 6, no. 2, pp. 28–33, 1959.

[9] Igor Podlubny, *Fractional Differential Equations*, Academic Press, 1999.

[10] I. Podlubny, "Fractional-order systems and $PI^{\lambda}D^{\mu}$ controller," *IEEE Trans. Automatic control*, vol. 44, no. 1, pp. 208–214, 1999.

[11] Y. Luo and Y. Q. Chen, "Fractional-order [proportional derivative] controller for a class of fractional order systems," *Automatica*, vol. 45, no. 10, pp. 2446–2450, 2009.

[12] H. S. Li, Y. Luo, and Y. Q. Chen, "A fractional order proportional and derivative (FOPD) motion controller: Tuning rule and experiments," *IEEE Transactions on Control Systems Technology*, vol. 18, no. 2, pp. 516–520, 2010.

[13] S. E. Hamamci and N. Tan, "Design of PI controllers for achieving time and frequency domain specifications simultaneously," *ISA Trans.*, vol. 45, no. 4, pp. 529–543, 2006.

[14] S. E. Hamamci, "Stabilization using fractional-order PI and PID controllers," *Nonlinear Dynamics*, vol. 51, pp. 329–343, 2008.

[15] C. H. Chang and K. W. Han, "Gain margins and phase margins for control systems with adjustable parameters," *J. Guid., Control, Dyn.*, vol. 13, no. 3, pp. 404C408, 1990.

[16] S.E. Hamamci, "An algorithm for stabilization of fractional-order time delay systems using fractional-order PID controllers," *IEEE Transactions on Automatic Control*, vol. 52, no. 10, pp. 1964–1969, Oct. 2007.

[17] N. Hohenbichler and J. Ackermann, "Synthesis of robust PID controllers for time delay systems," in *Proc. Eur. Control Conf.*, Cambridge, U.K., 2003, p. [CD ROM].

[18] J. Ackermann and D. Kaesbauer, "Stable polyhedra in parameter space," *Automatica*, vol. 39, no. 5, pp. 937–943, 2003.

[19] C. Hwang and Y. C. Cheng, "A numerical algorithm for stability testing of fractional delay systems," *Automatica*, vol. 42, no. 5, pp. 825–831, 2006.

[20] YangQuan Chen, "Impulse response invariant discretization of fractional order integrators/differentiators compute a discrete-time finite dimensional (z) transfer function to approximate s^r with r a real number," *Category: Filter Design and Analysis, MATLAB Central, http://www.mathworks.com/matlabcentral/fileexchange/ loadFile.do objectId=21342 objectType=FILE*, 2008.